EEG brain network study during resting states

Group 3: Pavan Kumar Alikana (1826777), Dastagiri Dudekula (1826239), Vamsi Gunturi (1794653)

Abstract:

This project focuses on understanding brain signal and connectivity patterns related to the eye states. More specifically, we analyzed brain Signals recorded by EEG for two different Eye states i.e. Eye open(EO) and Eye close(EC) respectively. We analyzed the 64-channel EEG signals from a single subject(S004) with eyes-open and eyes-closed baseline conditions. We did 4 types of analysis namely connectivity graphs, graph theory indices, motif analysis and community detection. More on this in their respective sections. At each stage of analysis, we emphasized arising differences between EO and EC states, accordingly concluded main identifiers of each state. To do this we focused on understanding the difference between the brain connectivity estimated with the MVAR estimation approaches like Partial directed coherence (PDC) and Direct Transfer Function (DTF) (the second one tends to give connectivity value little bit bigger than the first one). We also performed motif analysis using the tool mfinder and considering 3-node and 4-node motif configuration. We were able to obtain motifs and anti-motifs for the configuration with 3 and 4 nodes. We also to carried out specific analysis about information about the connection involved in a specific community detection configuration (modularity-based vs information theory-based approaches). Finally, after our observations while computing the community detection, we highlighted the weaknesses of Louvain's' algorithm in recognizing small communities compared to Info map.

Introduction:

Understanding brain functionality has been a major interest among the computational neuroscientists. Over the years different methodologies have been introduced and implemented to accomplish that. Electroencephalography (EEG) was invented in 1924 by German scientist Hans Berger and since then scientific interest to explain various human behavior and infer functional aspects of both normal and pathological brain processes with EEG has been strongly increasing. Not only different human behavior such as eye movement, attention and hand clenching can be visualized with EEG signals, but also human conditions such as schizophrenia or intelligence can be inferred from EEG signal data. All these states are associated with a particular frequency which aids us in understanding the functional behavior of complex brain structures. In this way, EEG allows us to acquire brain signals corresponding to various states. In this work, we have concentrated on determining differences in two particular states: eyes open (EO) and eyes closed(EC). We have studied 64-channels EEG signals, corresponding to a single subject (N=4). Then we performed spectral, connectivity, graph indices, motifs and community detection analysis by emphasizing arising differences between EC and EO at each stage.

1. Methods:

We downloaded the two EDF+ files corresponding to two 64-channels EEG signals from a single subject(S004). One signal was obtained with the subject at rest with EC, and the Other signal also at rest with EO. The two signals on one channel can be observed in Figure 1

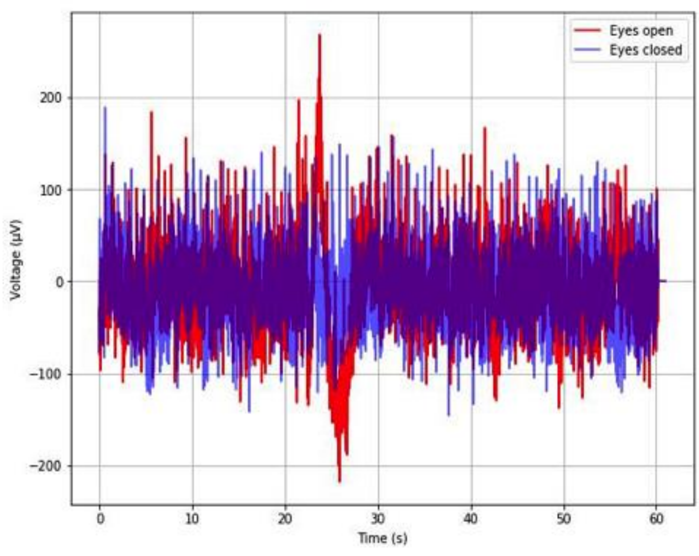

Figure 1: EEG signals for Eyes-open and Eyes-closed states

1.1 Connectivity graph:

The functional connectivity at the level of the brain structures (the connectivity derived from scalp EEG Measurements) can be estimated with the use of a spectral estimator based on the Multivariate Autoregressive Model (MVAR). In order to know the connectivity pattern in which the 64 channels are involved, we implemented both Direct Transfer Function (DTF) and Partial directed coherence(PDC) estimators, which measure the effect of a channel on another one(both direct and indirect) and only direct respectively.

Deciding on best frequency:

The estimations of connectivity between signals is executed first with the implementation of the MVAR. since this method requires the selection of the order for the model we used the Akaike information criterion for MVAR order estimation. We obtained best order for model to be 5 and 6 respectively for EO and EC states. Since the frequency spectrum of each channel is between 0-80Hz, we selected 80 as number of spectrum data points obtaining 80 connectivity matrices 64_64, each for a frequency band. The frequency selected is based on the waves that have range between 8-13 Hz, with an observed peak in 10 Hz in the estimation of the Power Spectral Density, as seen above in Figure 1. Hence the chosen matrix corresponds to the 10th frequency: on that matrix will be applied a threshold for the construction of the adjacency matrix: if the estimated effect of the channel on another is bigger than the threshold we consider connection between the two nodes, otherwise will be considered not connected. More details on this in the results section. We can see a graphical representation of the adjacency matrices for EC using DTF with 20% density in the Figure 2.1 and topology representation of EO state using PDC with density 5% in Figure 2.3

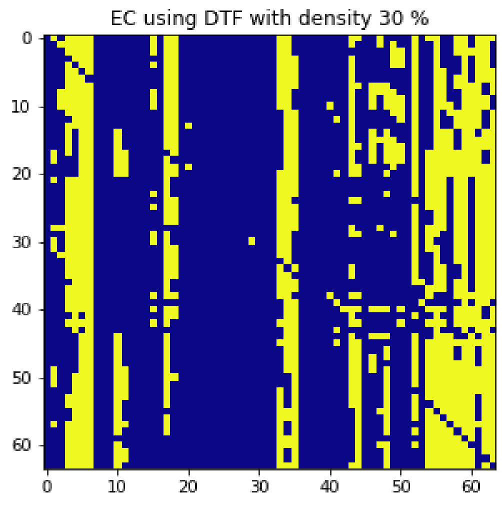

Figure 2.1: Binary adjacency matrix representation for Eyes closed using DTF with density 30%

Figure 2.2 shows the threshold (best alpha) representation of 4 different case i.e.., PDC EO, PDC EC, DTF EO and DTF EC for different density values like 1%, 5%, 10%, 20%, 30% and 50% respectively. More details on this in the results section

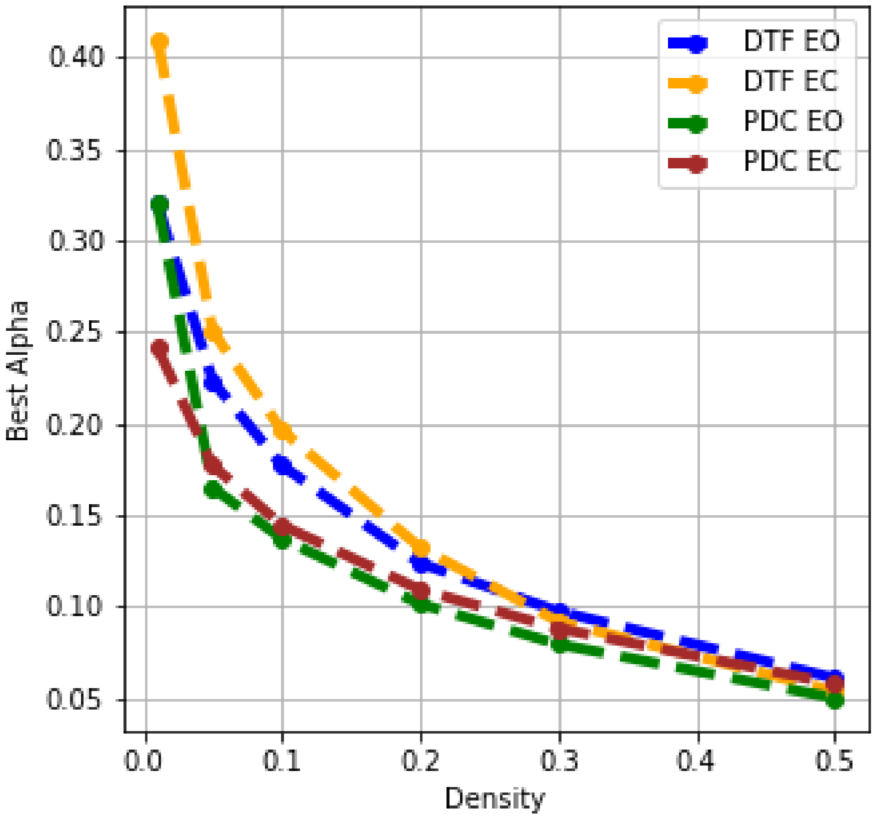

Figure 2.2: Best alpha vs Density for different states using PDC and DTF

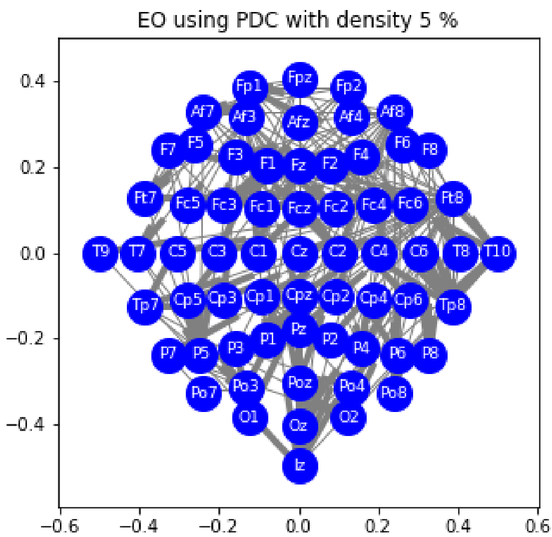

Figure 2.2: Topology representation of EO using PDC with graph density 5%

1.2 Graph theory indices:

Using networkx python package, we studied the structure of the PDC and DTF networks from a macroscopic point of view using two global indices: average clustering coefficient and average shortest path length and from a microscopical point of view using local indices we measured the total degree, In-degree and out-degree of each node. Correlation of global indices in different states using PDC and DTF are shown in Figure 3.1. More details about our analysis in results section.

The average clustering coefficient is defined as

$$C = \frac{1}{n}\sum_{i=1}^{n} Ci$$

where n is the number of all vertices and

$$Ci = \frac{|\{\mathrm{ejk} : \ \mathrm{vj}, \mathrm{vk} \exists \mathrm{Ni}, \mathrm{ejk} \exists \mathrm{E}\}|}{\mathrm{ki}(\mathrm{ki} - 1)}$$

also, k_i is the number of neighbors of a vertex,

e_i is the edge that connect vi with v_j,

Ni is the neighborhood of vi and E is the set of all edges.

The average shortest paths length is defined as

$$\mathrm{lg} = \frac{\sum_{i=1, i \neq j}^{n} d(\mathrm{viv\ j})}{\mathrm{n}(\mathrm{n} - 1)}$$

where $d(v_i, v_j)$ denotes the shortest distance between vertices i and j.

Small word network: A small word network in mathematical graph defines networks in which most nodes are not neighbors among themselves but at the same time most nodes are reachable from every other node by a small number of steps. This kind of organization lets a rapid integration of information between different specified brain areas even when they are distant

Topological representation of local indices is shown in Figures 3.1, 3.2 and 3.3

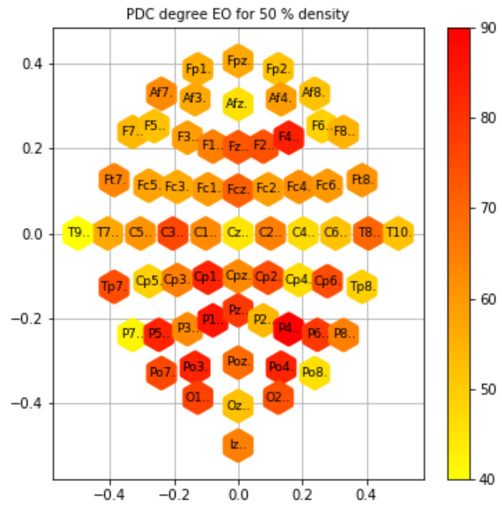

Figure 3.2: Degree of the nodes in EO state using PDC at 50% density

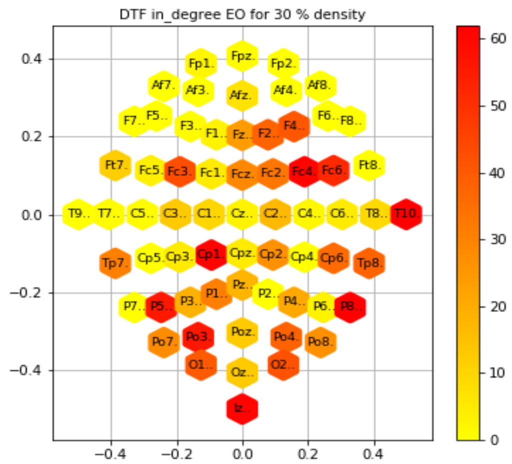

Figure 3.2: In degree of the nodes in EO state using DTF at 30% graph density

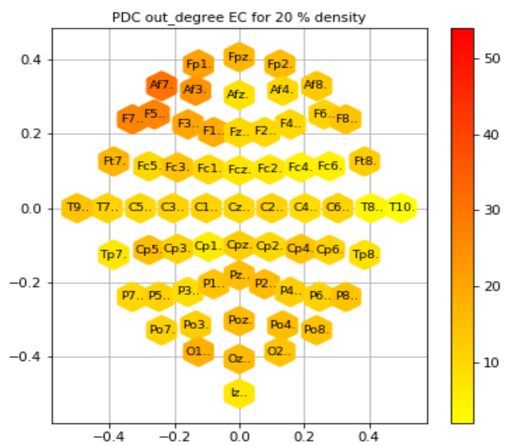

Figure 3.3: Out degree of the nodes in EC state using PDC at 20% graph density

1.3 Motif analysis

Network motifs are defined as patterns of interconnections occurring in complex networks at numbers that are significantly higher than those in randomized networks. Roughly speaking, in a network configuration we can define a motif a subnetwork that appear often in the real network more than would expected in a random network, assuming a statistical meaning. For the networks of both the resting conditions, EO and EC, we want to get the 3-nodes subgraph configuration and the relative frequencies and statistical significances for 3-node connected subgraph we have 13 possible combinations of configurations as shown in Figure 4.2 . Looking at the range of the appearance frequency for the random network (given by $\mu \pm \sigma$ of the frequency) we get the motif and anti-motif.

The subgraphs that appear more in the real network rather than the random one, are marked as motif and the subgraph that appear more in the random network rather than the real one, are marked as anti-motif. If the subgraphs have the frequency inside the interval of the random network, it means that the number of appearances in the real network is similar to a random network, so these subgraphs don’t have any significance.

We performed the motif analysis with the tool mfinder2, the results are showed for both the rest conditions respectively. If we want to do an analysis considering only a type motif pattern, with the use of the tool mfinder we can obtain all the subgraphs of the original network that have the configuration desired. A graphical representation with this configuration. A different interesting analysis can be done with the detection of 4-node connected subgraph, following the same procedure as above. Since in this case the motifs combinations are 199, we are going to show only the significant results, in particular the 10 subgraphs with higher frequency. More details on motifs in results section.

1.4 Community detection:

To detect communities, we used the Louvain algorithm which is modularity based and it was performed in two steps. First, it iterates through all the nodes in the network and assigns each node to a community as long as it increases the modularity. Afterwards, super nodes are created from the clusters of the first step and the process is repeated again until convergence.

Unfortunately, this algorithm is not implemented for directed networks on networkx, so we used instead the igraph python library, where it is implemented.

2. Results and Observations

2.1 Connectivity graph:

In order to estimate functional brain connectivity among the 64 channels, we used both MVAR estimators PDC and DTF. We dynamically calculated threshold (best alpha) for all densities mentioned in the problem statement i.e.., 1%, 5%, 10%, 20%, 30% and 50% so that we have a holistic analysis on different observations based on the parameters chosen (state, method and density). Full results can be found in Appendix A in Figure 5.1, 5.2, 5.3, 5.4 where we tried to show a topographical representation for all the 64 channels. For adjacency matrix representations please refer to Figures 5.5, 5.6,5.7, 5.8 in Appendix A

As we can see in the Figures 5.3, 5.4 with PDC estimator (two top subfigures), when the subject is in EC state we can observe that approximately 50% of the connection remains the same and the rest is changing. It seems like the network is becoming more concentrated around parietal central channels.

Since DTF is taking into account also indirect influence, it is reasonable to observe more connections in the network on the Figure 5.1 and 5.2 for DTF than topologies based on PDC in 5.3 and 5.4. Here, we see even more obvious concentration around central parietal channels than before.

2.2 Graph theory indices

To analyze patterns in the graphs created in the previous step we did both microscopic and macroscopic analysis using host of indices both at the graph level (global) and at the individual node level(local).

For local indices, we tried to do all this analysis using both PDC and DTC and apply them to all the graphs with densities 1%, 5%, 10%, 20%, 30% and 50%. Full results are included in Appendix B in Figures 9,10,11,12 (for degree), Figures 13,14,15,16(for in-degree) and Figures 17,18,19,20 (for out-degree)

For global indices, we tried to compare both clustering coefficient and average shortest path from both PDC and DTF at all densities. The plots for this are included above in the Figure 3.1.

We observed that average shortest path length shows a regular behavior, it decreases regularly as we increase the network density. This is true for both eyes open and close states for both PDC and DTF estimators

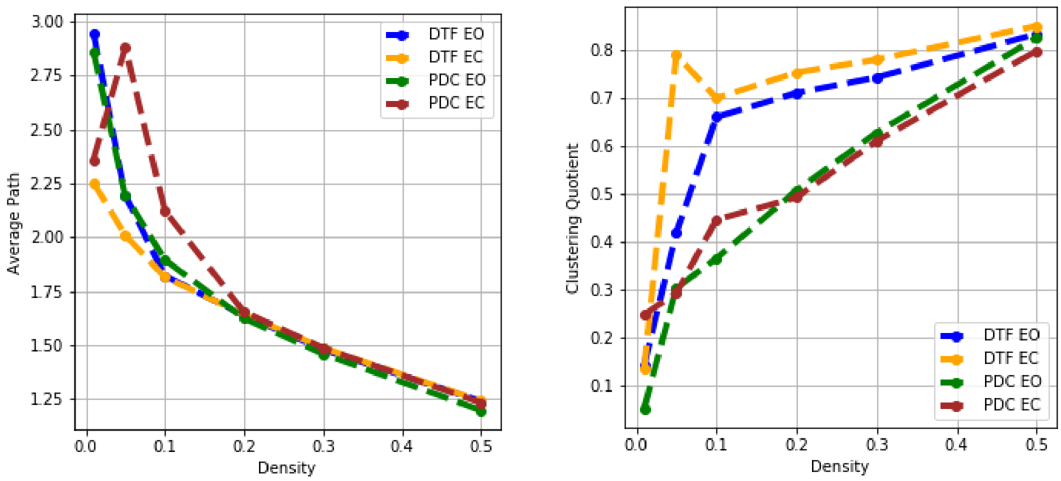

Figure 4.1: Global indices observed in states EO and EC using PDC and DTF at different densities

An interesting observation that we made from above figure 3.1 is that increasing density does not always lead to increasing clustering coefficient (on interval from 10 to 15%). This effect takes place probably because the neighborhood of a single node is becoming bigger while interconnections inside the neighborhood are increasing more slowly and hence the average clustering coefficient is not keeping up with the increase in graph density. We also observed that PDC based networks tend to show less connectivity while between two PDCs(or two DTF networks) the most connected is the one that was built based on eyes closed dataset.

From the degree and in-degree topologies of both PDC and DTF in Appendix B Figures 9,10,11,12,13,14,15,16 we observed that the degree coefficients remain the same for both PDC and DTF (for both eyes open and eyes closed) but we observed a rich get's richer phenomenon for degree topologies based on PDC.

For out-degree topologies of both PDC and DTF in Appendix B Figures 17,18,19,20 we observed rather contrasting phenomenon ie.., DTF has more of nodes having more out degree than that of nodes based on PDC.

For correlating local indices as shown in Fig 5.21 in Appendix B we used the data of the highest degree node for a given graph (DTF EO, EC and PDC EO, EC). We observe that degree and outdegree remains the same for both EO and EC using PDC and DTF but there is a variation of in degree value across PDC and DTF across states (EO and EC)

Note: Tables for local indices and global indices for both PDC and DTF can be found in python notebook with name S004-Connectivity-Graph

2.3. Motifs analysis

3-node motifs analysis

All possible 3-nodes motifs are represented in the Figure 11.

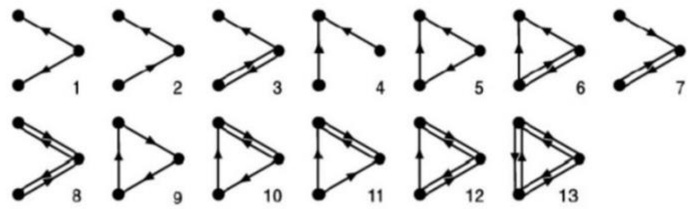

Figure 4.2: All possible 3-node motifs

The results on the described network are reported in the table below (motifs IDs are corresponding to the Figure 11). As we can see. most of the motifs are represented in both of the networks and now we can test if any of them are over-represented or appear to be anti-motifs.

For anti-motifs search we have fixed a threshold equal to 0.5 which means that a motif counts as anti-motif only if

$$0.5 * f_{\text{random}}(Gk) > f_{\text{original}}(Gk)$$

3 node motif type	F-EO	F-EC	statistical significance
S1: [(2 → 1),(2 → 3)]	196	434	under-represented
S2: [(2 → 1),(3 → 2)]	565	718	normal-represented
S3: [(2 → 1),(2 ↔ 3)]	46	60	under-represented
S4: [(2 → 1),(3 → 1)]	8251	7974	under-represented
S5: [(3 → 1),(2 → 1),(2 → 3)]	1256	1715	over-represented
S6: [(3 → 1),(2 → 1),(2 ↔ 3)]	88	131	over-represented
S7: [(1 → 2),(2 ↔ 3)]	1746	1462	normal-represented
S8: [(1 ↔ 2),(2 ↔ 3)]	33	53	under-represented
S9: [(1 → 2),(2 → 3),(3 → 1)]	6	10	normal-represented
S10: [(1 ↔ 2),(2 → 3),(3 → 1)]	108	81	under-represented
S11: [(1 ↔ 2),(3 → 2),(3 → 1)]	1479	1098	normal-represented
S12: [(3 → 1),(1 ↔ 2),(2 ↔ 3)]	240	181	normal-represented
S13: [(1 ↔ 2),(2 ↔ 3),(1 ↔ 3)]	128	65	over-represented

Note: we used DTF graph with density 20% to generate these 3-node motifs

Graphs for 3 node motif analysis can be found in Appendix C Figures 21 and 22

4-nodes motifs

Due to a wide range of all possible 4 nodes directed graphs, we will list here results only for over- represented motifs. We performed analysis regarding anti-motifs as well, but there was not any 4-nodes motif that would have at least twice bigger frequency in random networks compared to the original one. Results for 4 node motifs can be found in motif4 folder in data/motifs folder(full path data/motifs/motif4) in our submission.

2.4 Community detection

For community detection we used DFT graphs generated for EO and EC with density 20%. We applied both Louvain and Infomap approaches for detecting the communities in the above 2 graphs. Below are the topology diagrams for both cases.

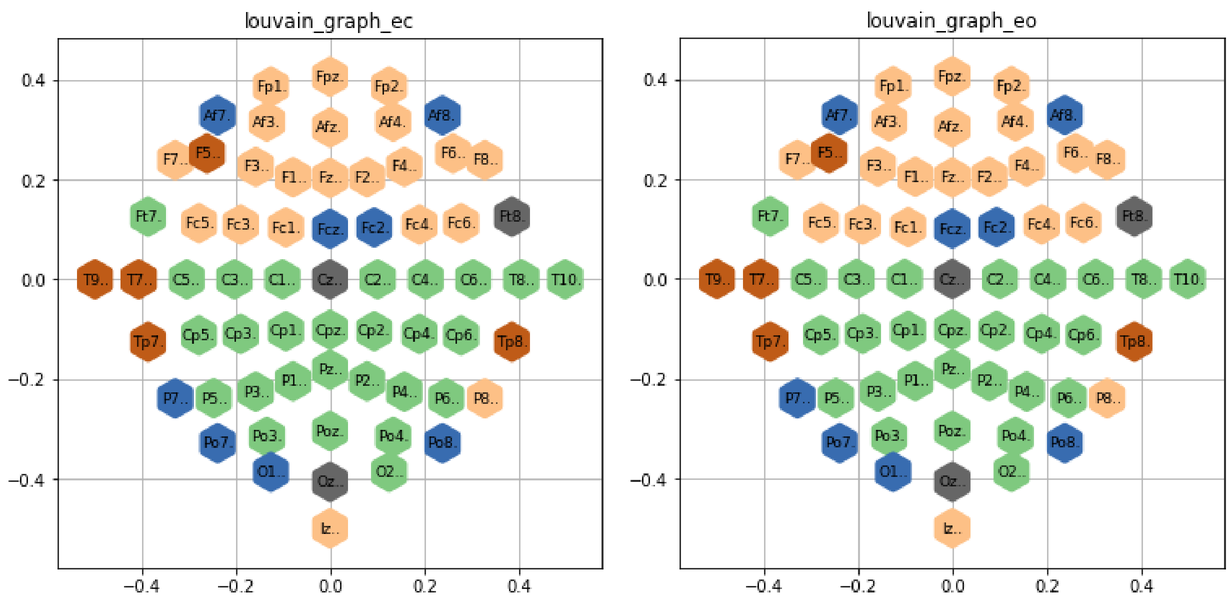

Figure 5.1: Topology diagram for community detection of DTF EO and EC for 20% graph density using Louvain

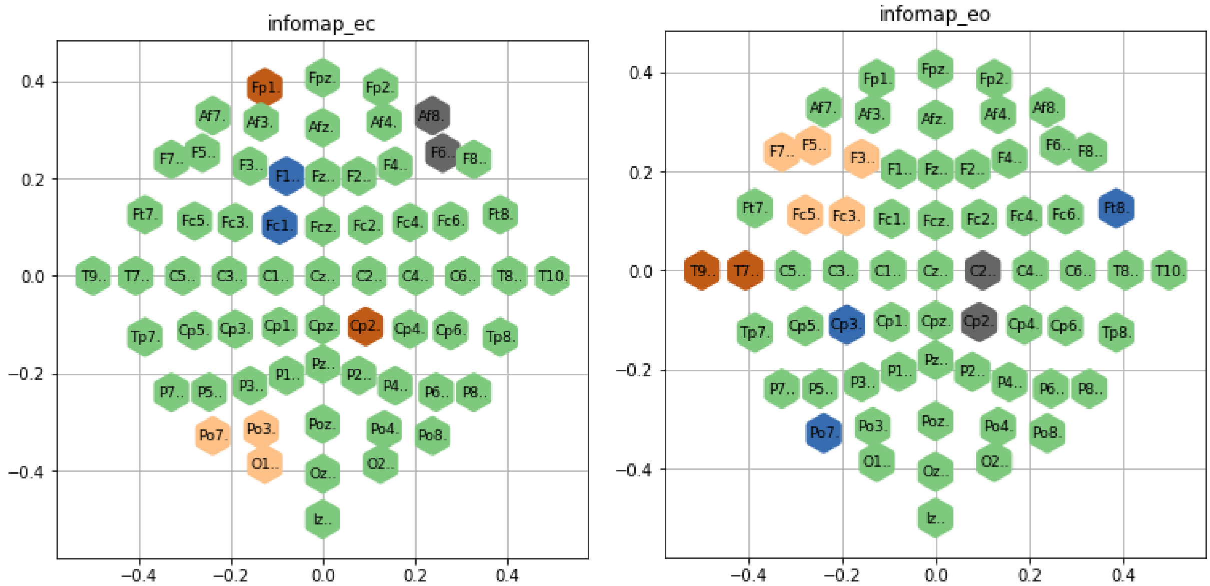

Figure 5.1: Topology diagram for community detection using DTF EO and EC for 20% graph density using Info map

For above DTF network using Louvain, we found 4 communities for state EC and 7 communities for state EO. The list of channels on each community can be found on Tables 1 and 2 on the Appendix D.

For above DTF network using Info map, we found 5 communities for state EC and 6 communities for state EO. The list of channels on each community can be found on Tables 3 and 4 on the Appendix D.

Overall, we observed that Info map does a better job in detecting the communities since the community detection of channels using Info map is far better than the community detection using Louvain algorithm. So, it is obvious to state the weaknesses of Louvain's' algorithm in recognizing small communities compared to Info map implementation.

3. Conclusion:

After analyzing the EEG signals from a single subject with eyes-open and eyes-closed baseline conditions in various perspectives we found significant differences that may be taken into account while working with these base-lines. First of all, basic signal analysis showed that a frequency of 10 Hz explains the most significant difference between the two baselines. Moreover, different MVAR estimators to build the network of EEG signals can lead to very different graphs, and an estimator that involves only direct interactions seem to generate a topology where communities are physically close in the brain.

Finally, in order to be more confident about the archived results in further research we would suggest examining data from several subjects and thus we would be able to determine statistical significance of all the differences listed above from all possible view points. Also, we strongly believe that specific analysis for motifs and community detection considering both DTF and PDC for all densities and 2 states would lead to further interesting insights about the patterns in signal data. We did the motif analysis and community detection using only DTF estimator with 20% graph density. We also want to state that by doing connectivity graph analysis and graph theory indices using above ideology has yielded us better correlations for comparing and contrasting different cases because as someone stated that a picture speaks a thousand words. By this we want to conclude our report.

Below are the tasks covered in our work:

Task	Class
1.1	Mandatory
1.2	A
1.3	A
1.4	D
1.5	C
2.1	Mandatory
2.2	D
2.3	B
2.4	C
2.5	B
3.1	Mandatory
3.2	C
3.4	E
4.1	Mandatory
4.2	B
4.3	C

Bibliography:

[1] Millet, David (2002). ”The Origins of EEG”. International Society for the History of the Neurosciences (ISHN)

[2] Karson CN, Coppola R, Daniel DG, Weinberger DR. Computerized EEG in schizophrenia. Schizophr Bull. 1988;14:193–197

[3] Thatchera RW, Northa D, Biver C. EEG and intelligence: Relations between EEG coherence, EEG phase delay and power. Clin Neurophysiol. 2005;116:2129–2141

[4] Alexandre Gramfort, Partial Directed Coherence and Direct Transfer Function using MVAR processes, Github repository: https://gist.github.com/agramfort/9875439

[5] Goldberger AL, Amaral LAN, Glass L, Hausdorff JM, Ivanov PCh, Mark RG, Mietus JE, Moody GB, Peng C-K, Stanley HE. PhysioBank, PhysioToolkit, and PhysioNet: Components of a New Research Resource for Complex Physiologic Signals. Circulation 101(23):e215-e220 [Circulation Electronic Pages; http://circ.ahajournals.org/cgi/content/full/101/23/e215]; 2000 (June 13). https://physionet.org/physiobank/database/eegmmidb/

[6] Scipy signal processing Version 1.0.0 https://docs.scipy.org/doc/scipy/reference/signal.html

[7] Lowry, Richard. ”Concepts and Applications of Inferential Statistics” http://vassarstats.net/textbook/ch12a.html

[8] Emmons S, Kobourov S, Gallant M, Borner K. Anal- ¨ ysis of Network Clustering Algorithms and Cluster Quality Metrics at Scale. Dovrolis C, ed. PLoS ONE. 2016;11(7):e0159161. doi:10.1371/journal.pone.0159161

[9] Vincent Traag, Louvain igraph, (2017), GitHub repository, https://github.com/vtraag/louvain-igraph

[10] Barry R. J., Clarke A. R., Johnstone S. J., Magee C. A., Rushby J. A. (2007). EEG differences between eyes-closed and eyes-open resting conditions. Clin. Neurophysiol. 118 2765–2773. 10.1016/j.clinph.2007.07.028

[11] Milo, R. (2002). Network Motifs: Simple Building Blocks of Complex Networks. Science, 298(5594), pp.824- 827.

[12] EEG Motor Movement/Imagery Dataset https://physionet.org/physiobank/database/eegmmidb/

[13] NETWORK MOTIF SOFTWARE https://www.weizmann.ac.il/mcb/UriAlon/download/network-motif-software

[14] Photocollage https://www.photocollage.com/

[15] Sergio Ballesteros, Olga Lazareva "Brain Oscillatory and Network Activity duringresting states” https://www.dropbox.com/s/g4mzis1syi2vyil/Ballesteros_Lazareva_EEG_Analysis.pdf?dl=0

[16] Pyedflib library: read/write EDF+/BDF+ files based on EDFlib Github repository:https://github.com/holgern/pyedflib

[17] Network motifs https://www.cs.helsinki.fi/u/lmsalmel/bio-models/NetworkMotifs.html

[18] ConnectiviPy https://connectivipy.readthedocs.io/en/latest/tutorial.html

Appendix:

Appendix A: Connectivity graph

Topology diagrams using DTF:

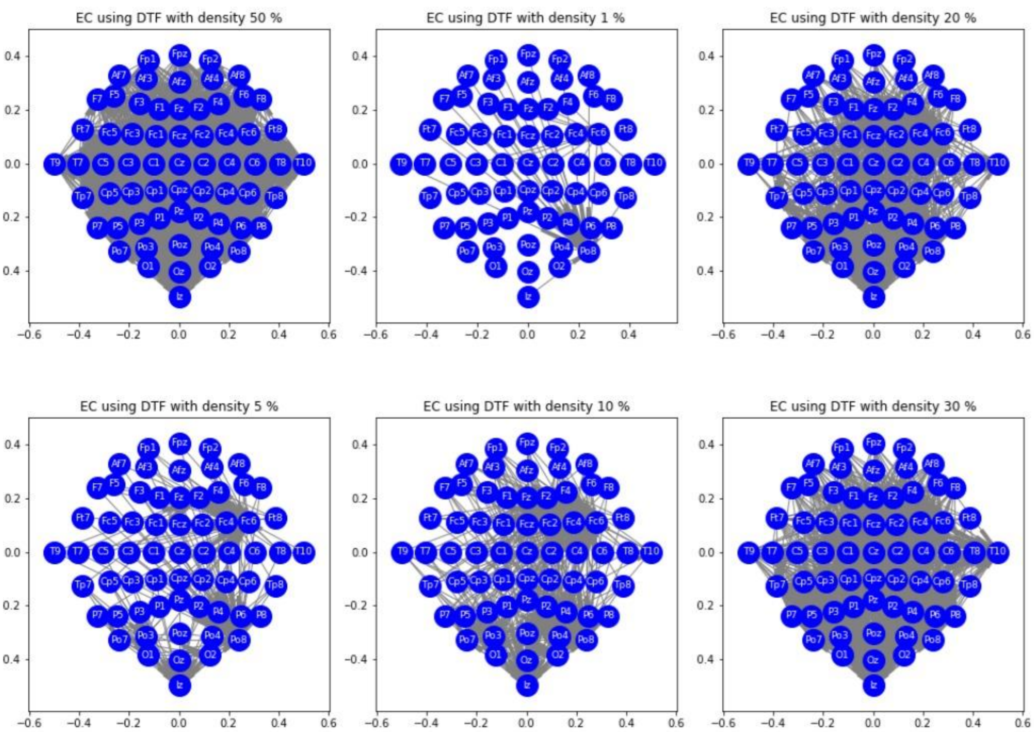

Fig 5.1: Topology representation for DTF EC at different densities

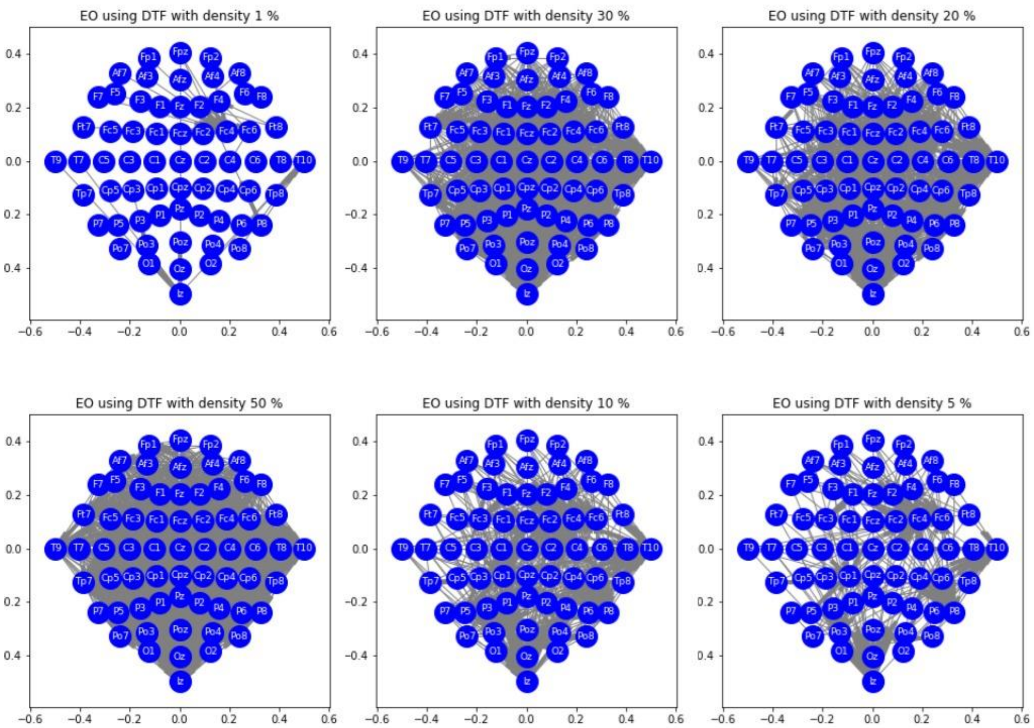

Fig 5.2: Topology representation for DTF EO at different densities

Topology diagrams using PDC:

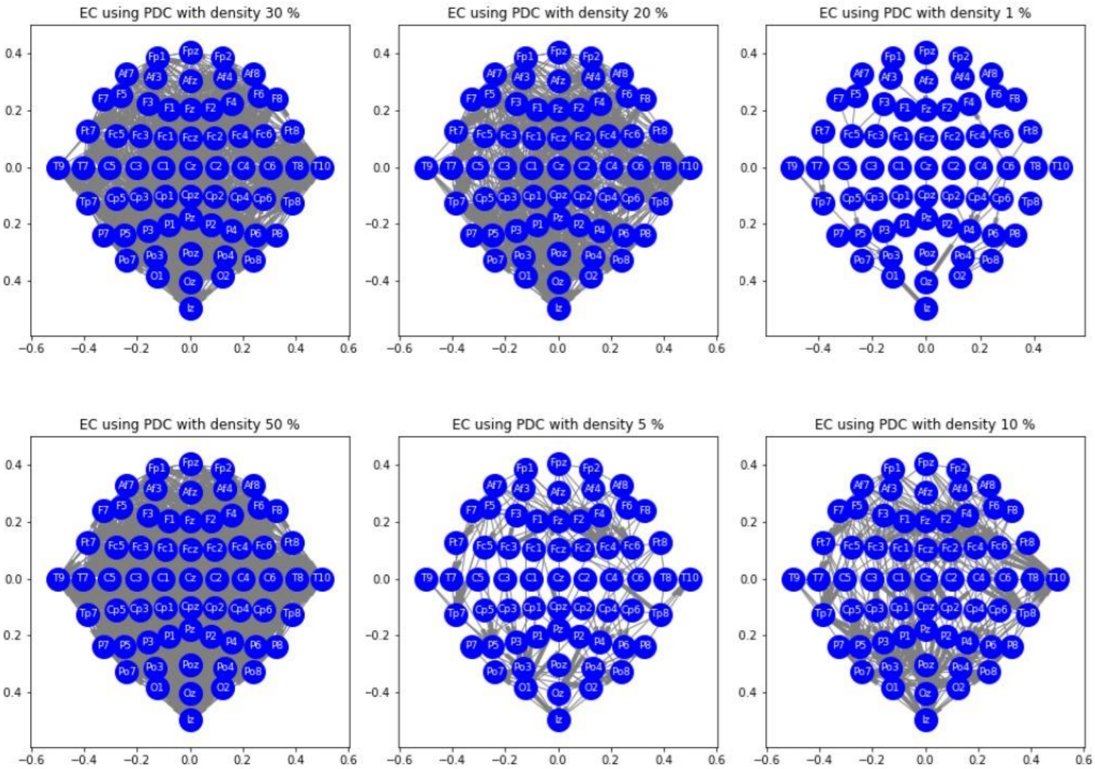

Fig 5.3: Topology representation for PDC EC at different densities

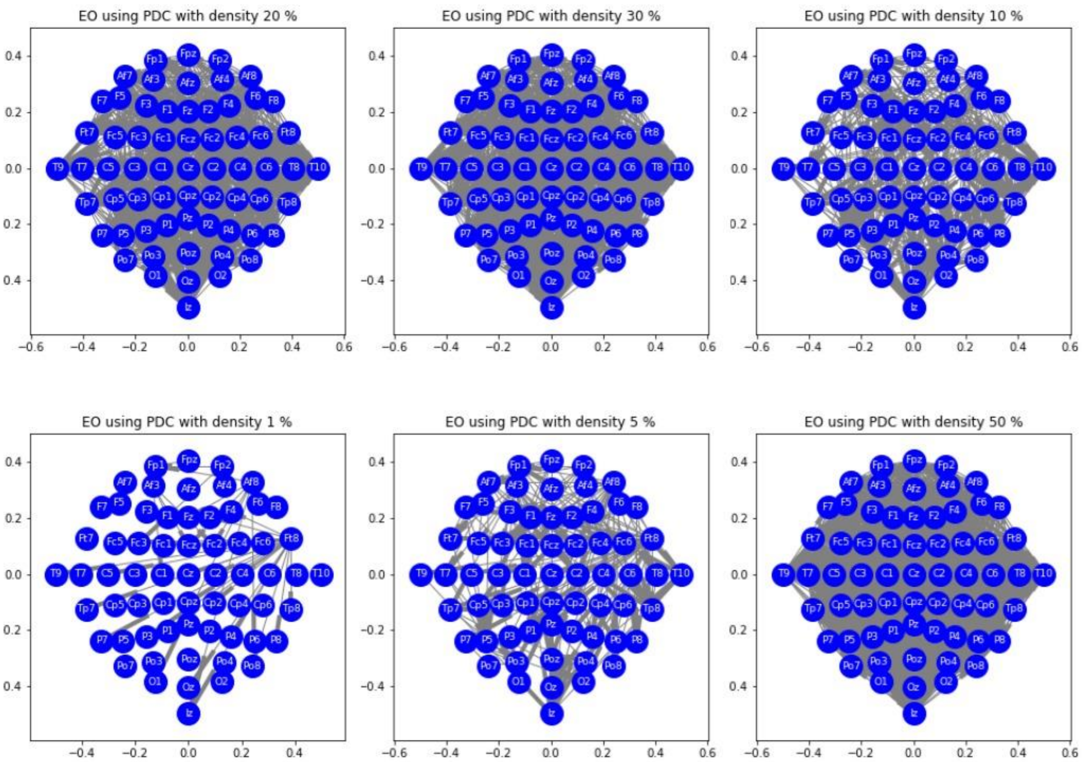

Fig 5.4: Topology representation for PDC EO at different densities

Adjacency matrix diagrams using DTF:

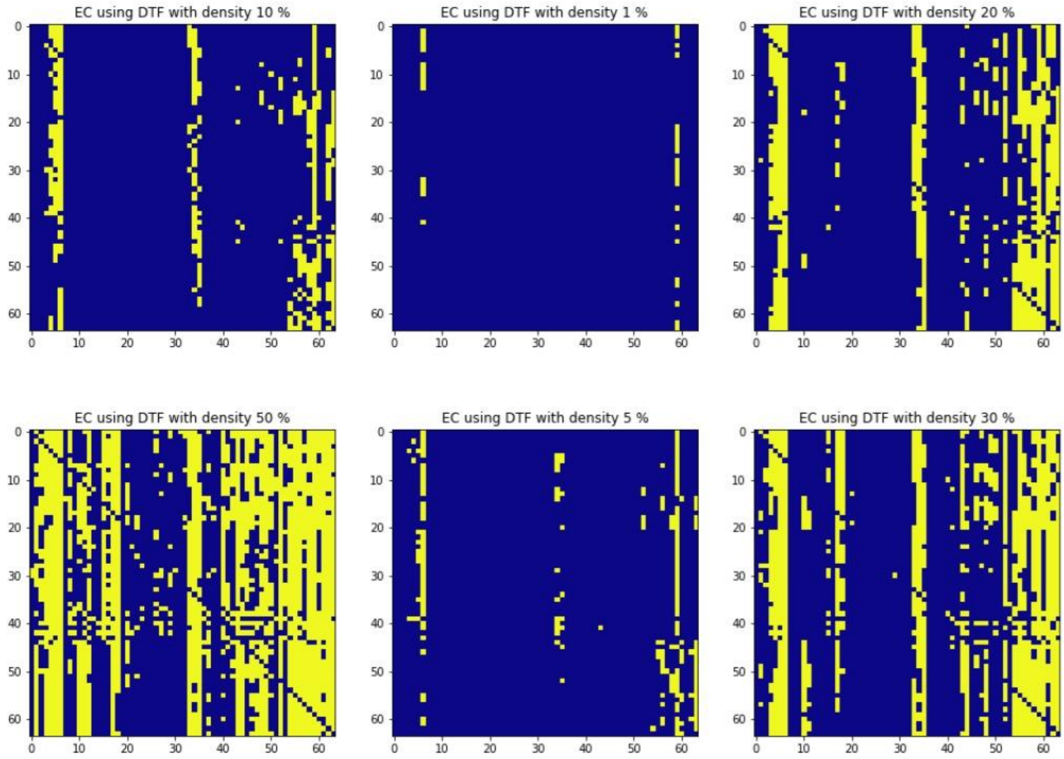

Fig 5.5: Adjacency matrix representation for DTF EC at different densities

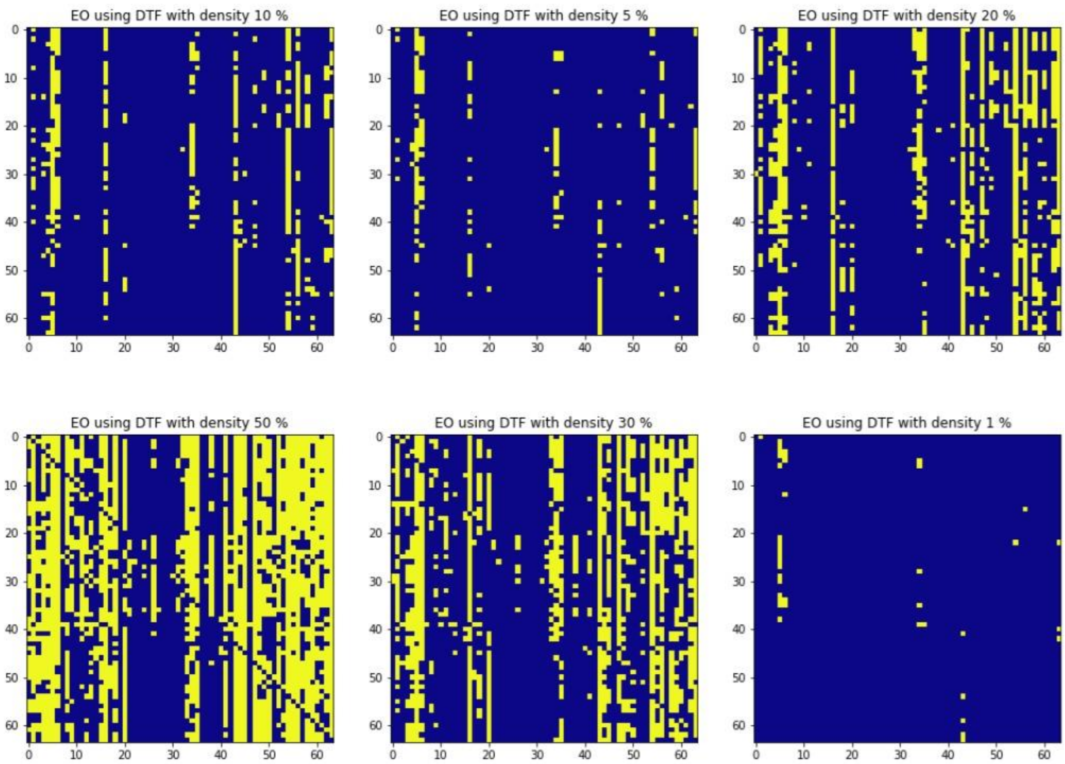

Fig 5.6: Adjacency matrix representation for DTF EO at different densities

Adjacency matrix diagrams using PDC:

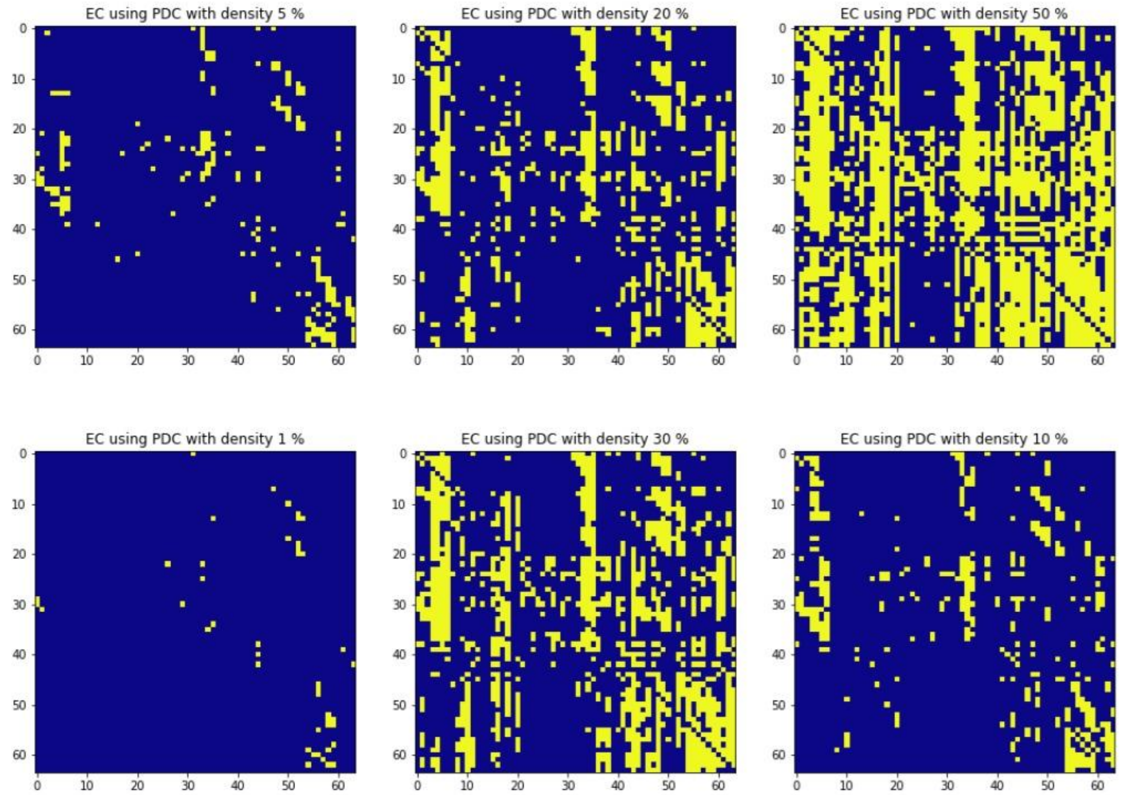

Fig 5.7: Adjacency matrix representation for PDC EC at different densities

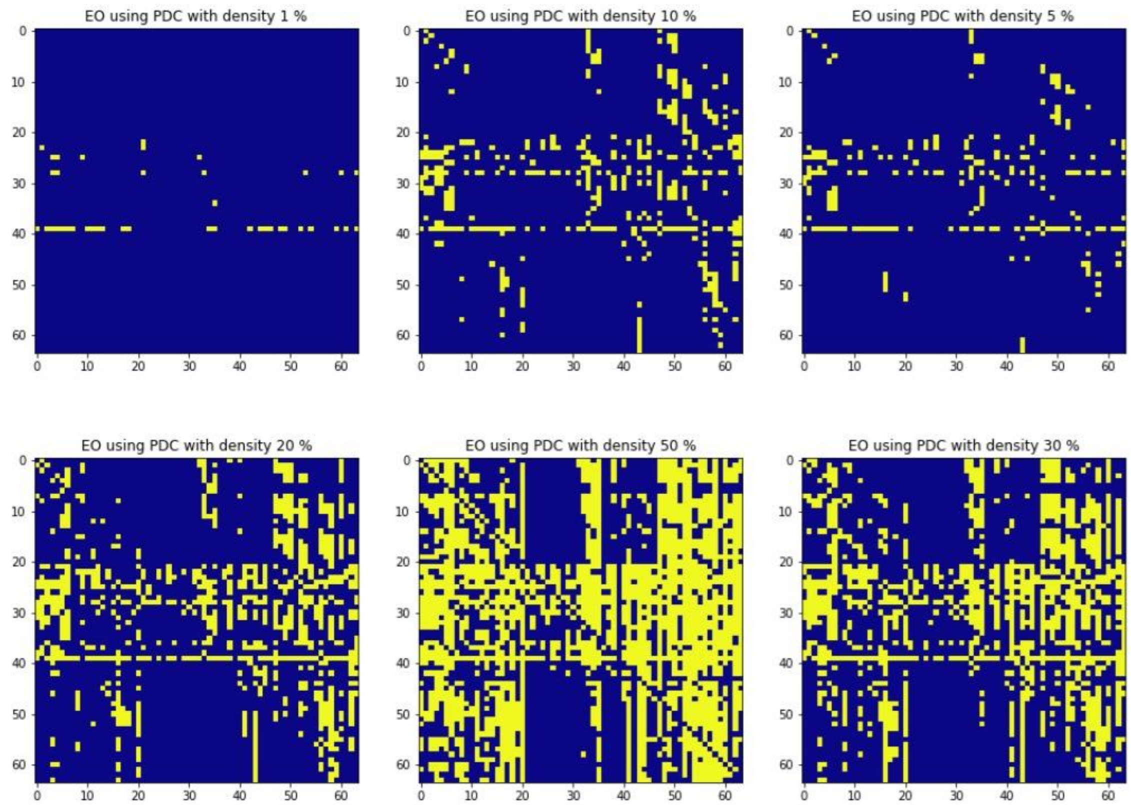

Fig 5.8: Adjacency matrix representation for PDC EO at different densities

Appendix B: Graph Indices

Degree topology diagrams using DTF:

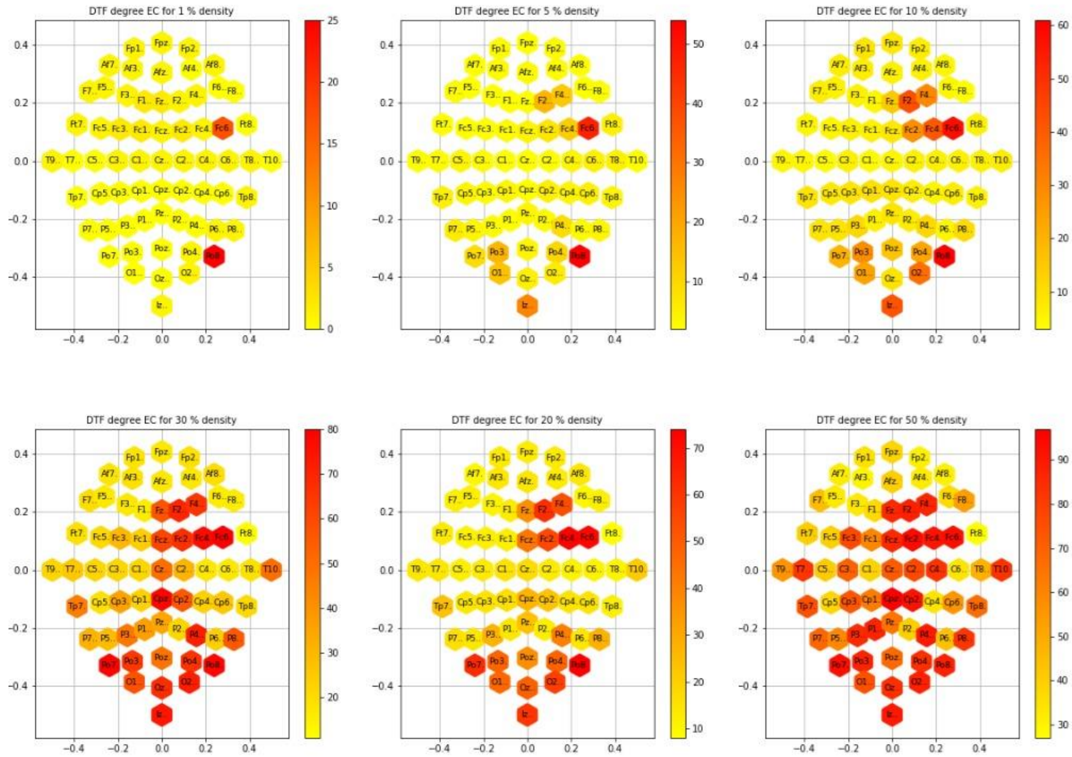

Fig 5.9: Topology representation of degree for DTF EC at different densities

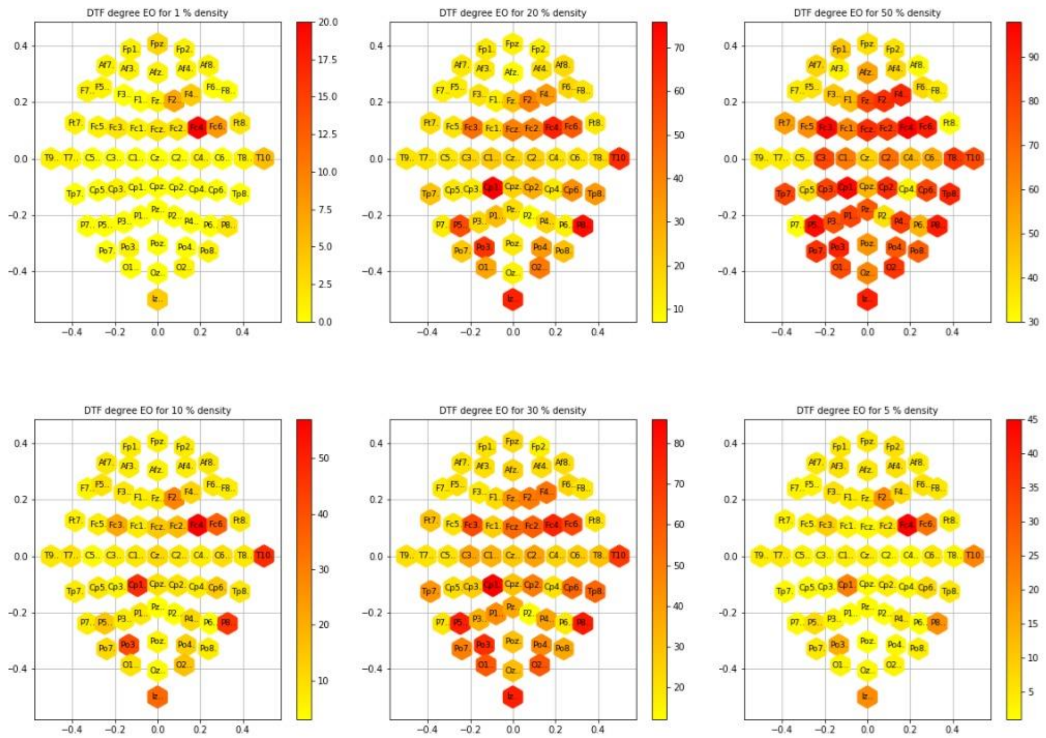

Fig 5.10: Topology representation of degree for DTF EO at different densities

Degree topology diagrams using PDC:

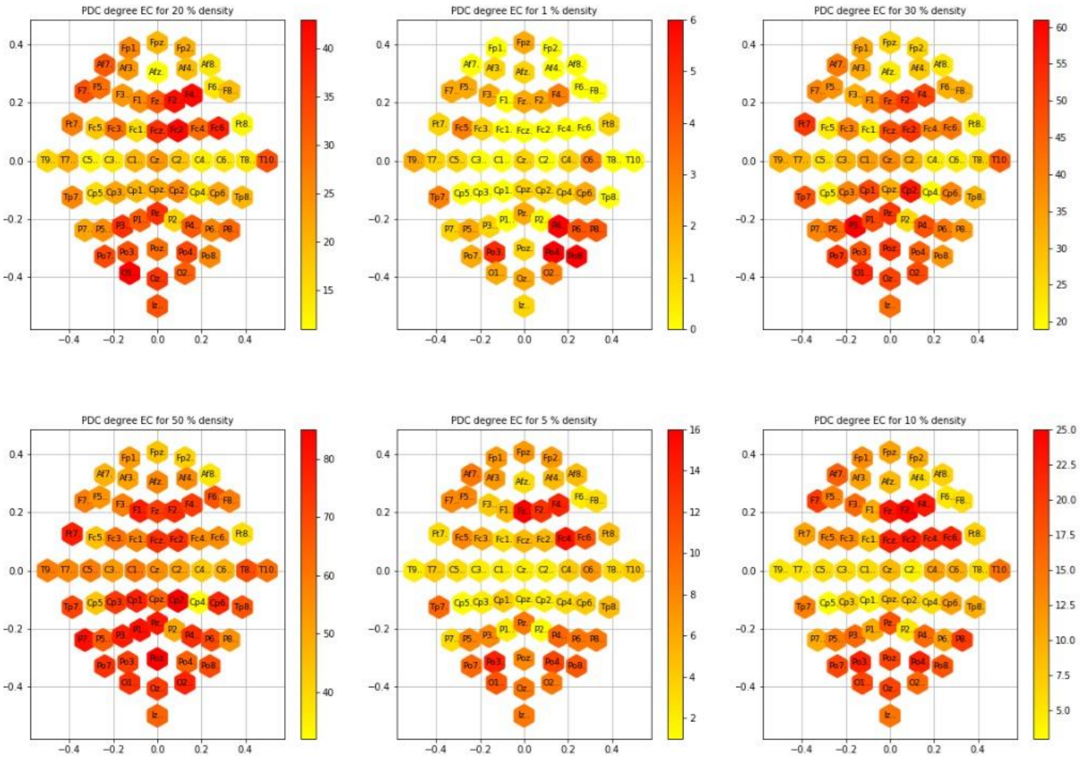

Fig 5.11: Topology representation of degree for PDC EC at different densities

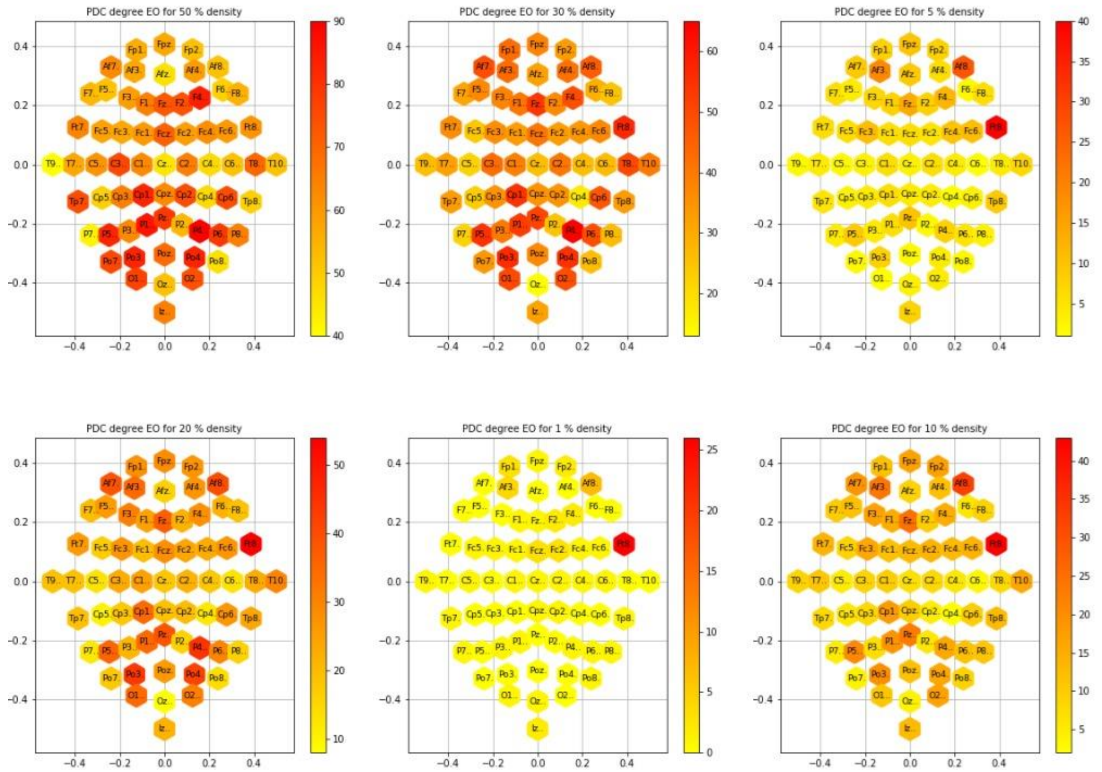

Fig 5.12: Topology representation of degree for PDC EO at different densities

In-Degree topology diagrams using DTF:

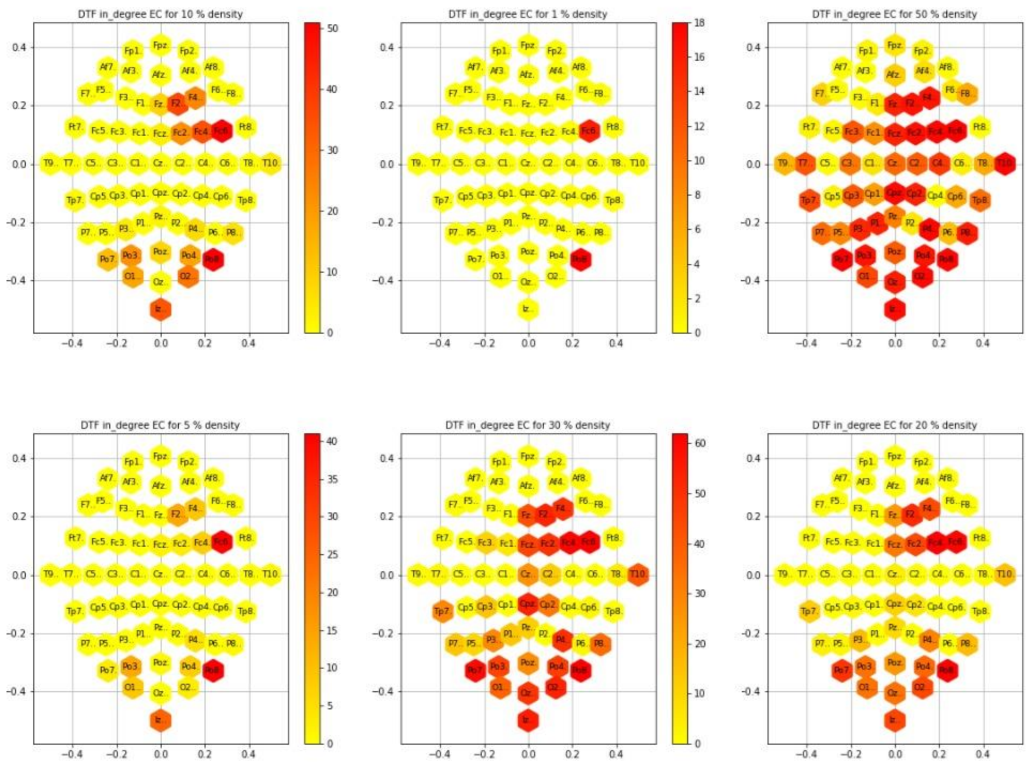

Fig 5.13: Topology representation of in-degree for DTF EC at different densities

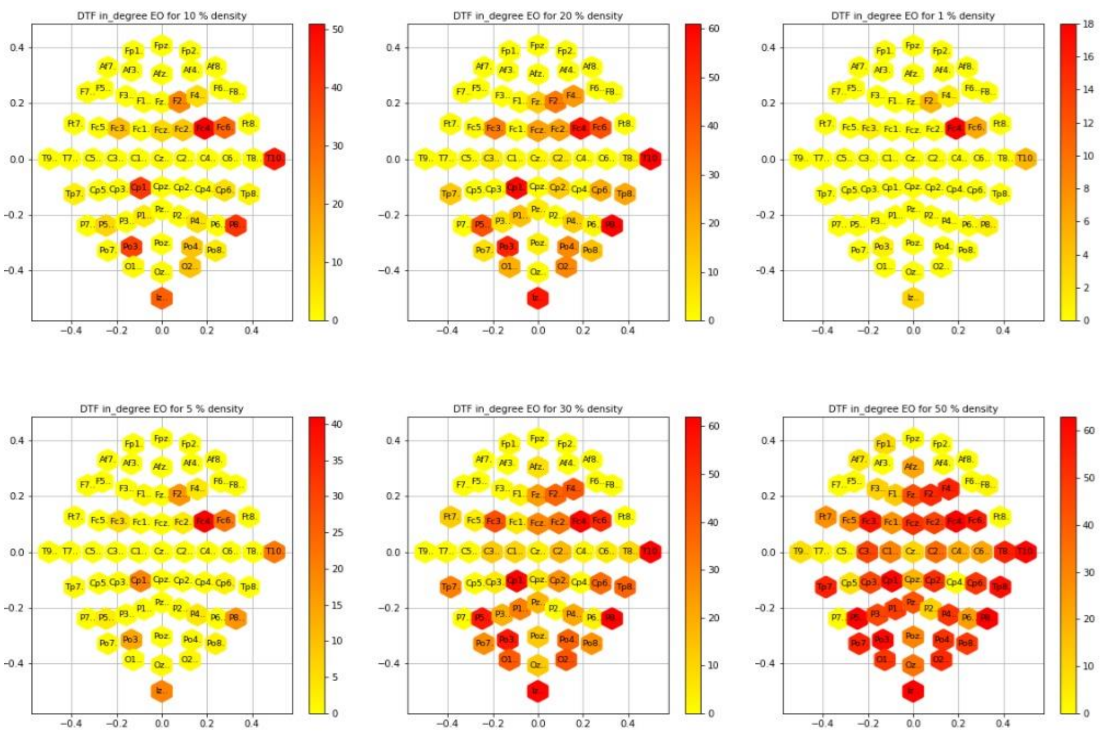

Fig 5.14: Topology representation of in-degree for DTF EO at different densities

In-Degree topology diagrams using PDC:

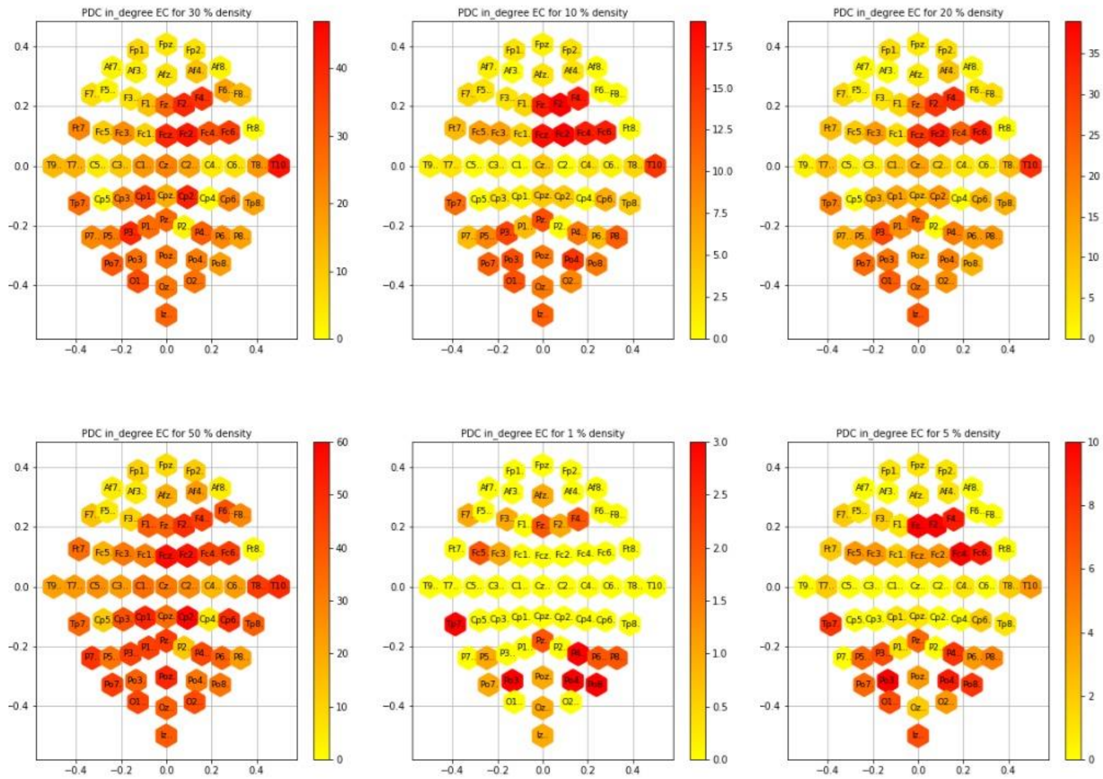

Fig 5.15: Topology representation of in-degree for PDC EC at different densities

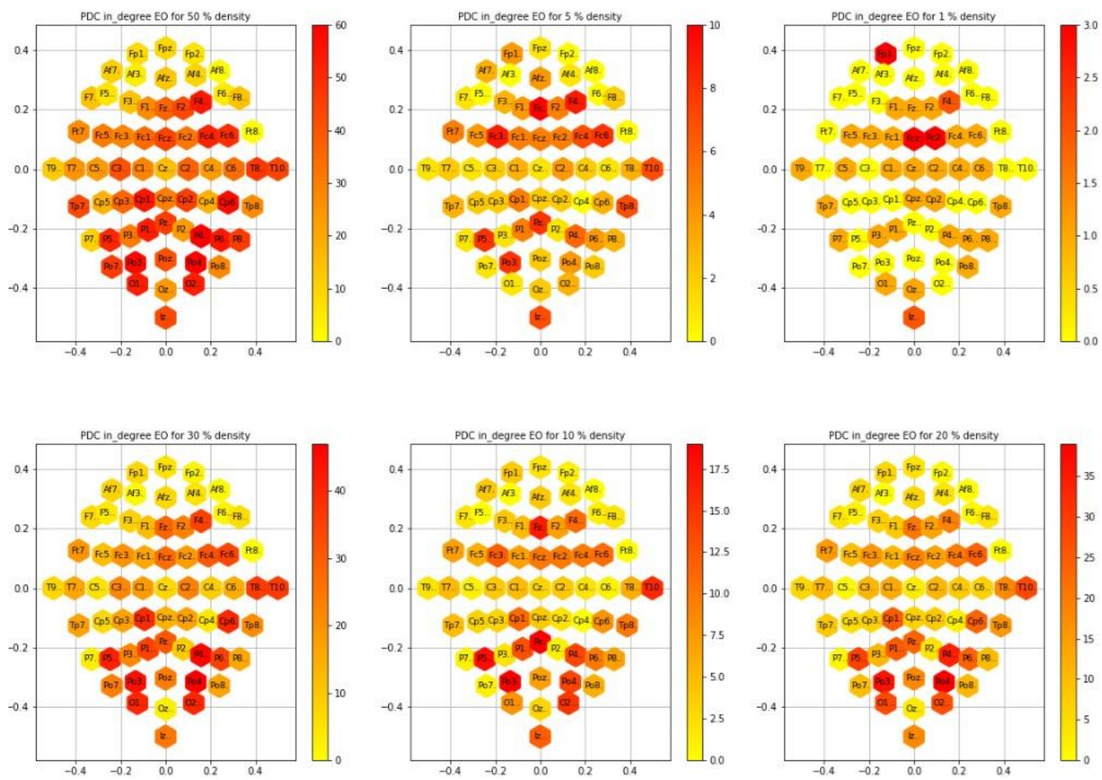

Fig 5.16: Topology representation of in-degree for PDC EO at different densities

Out-Degree topology diagrams using DTF:

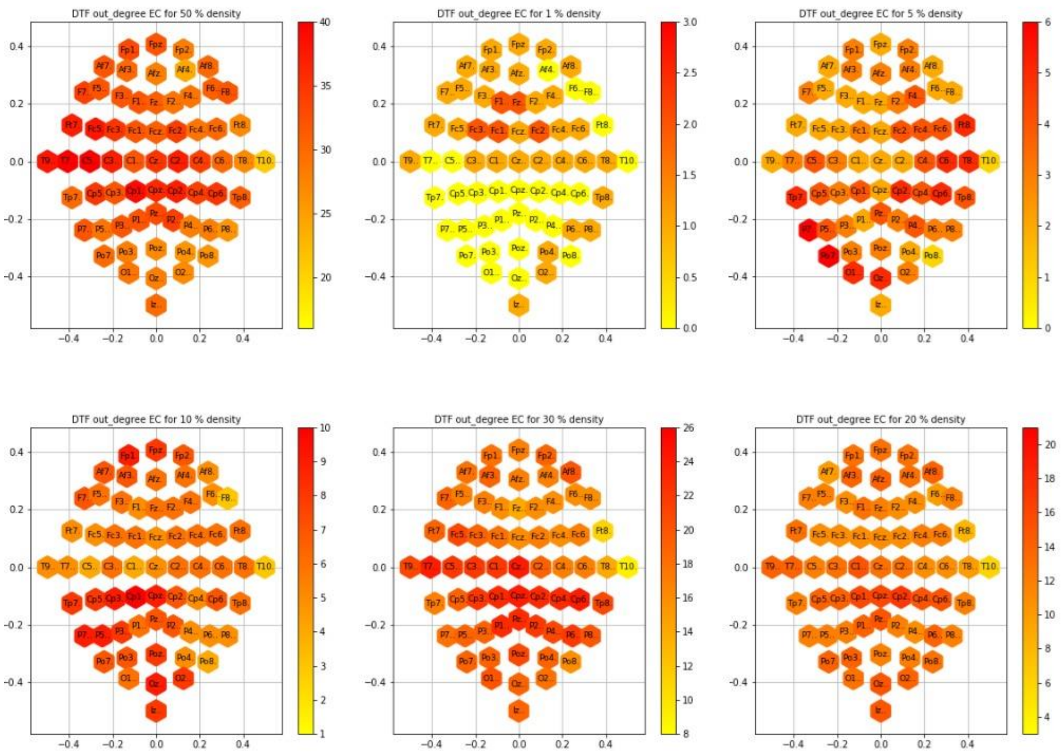

Fig 5.17: Topology representation of out-degree for DTF EC at different densities

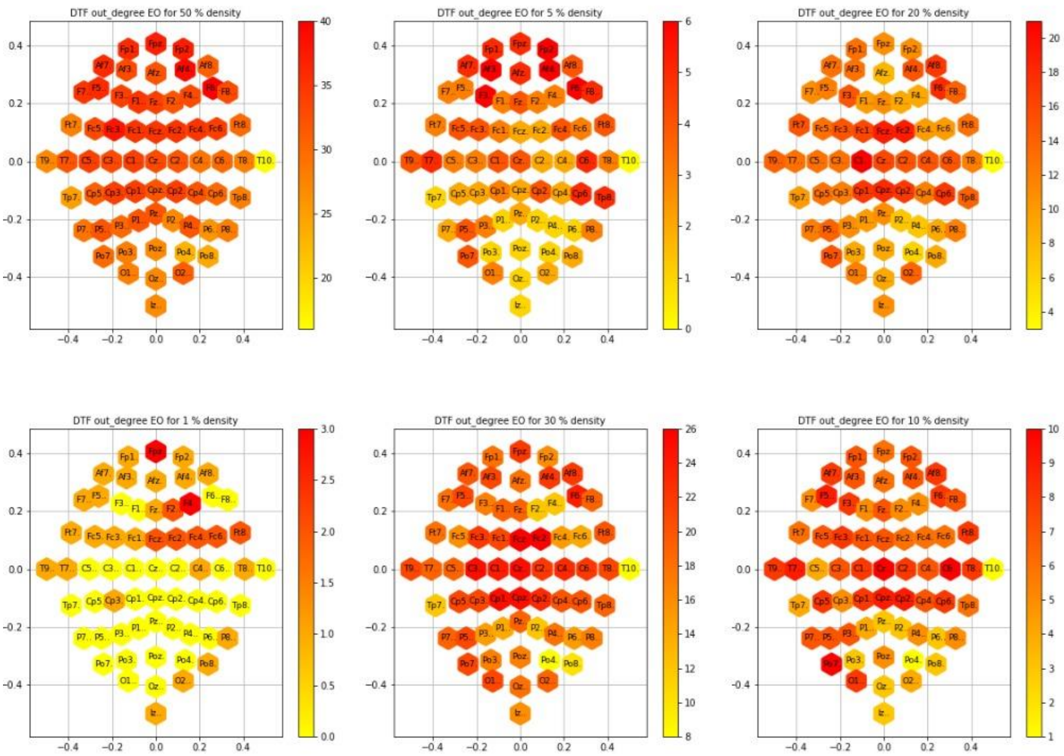

Fig 5.18: Topology representation of out-degree for DTF EO at different densities

Out-Degree topology diagrams using PDC:

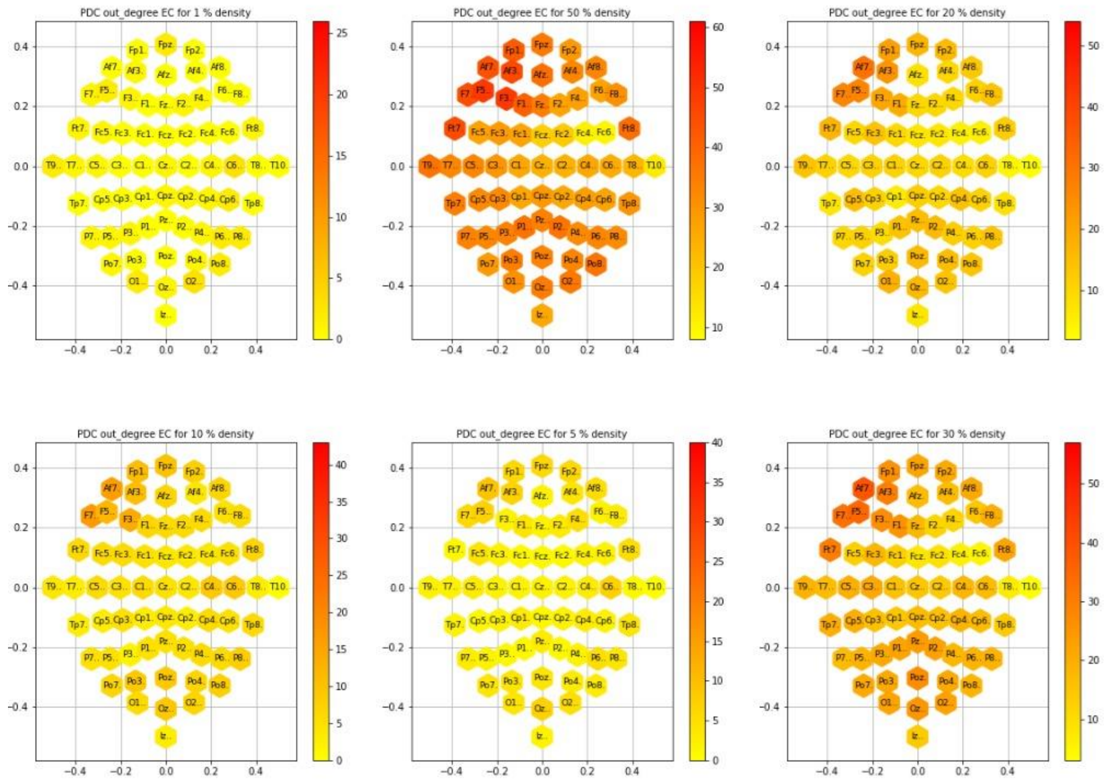

Fig 5.19: Topology representation of out-degree for PDC EC at different densities

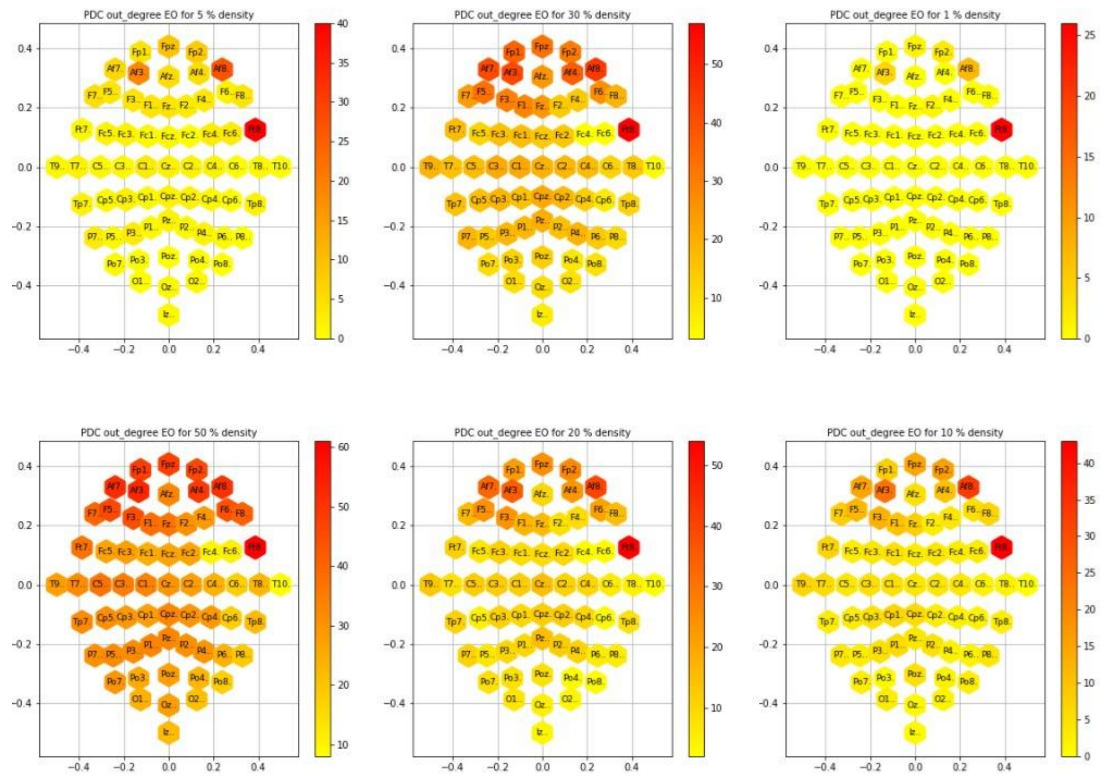

Fig 5.20: Topology representation of out-degree for PDC EO at different densities

Correlation of Degree, In-Degree-Out-degree across PDC and DTF (both EO and EC)

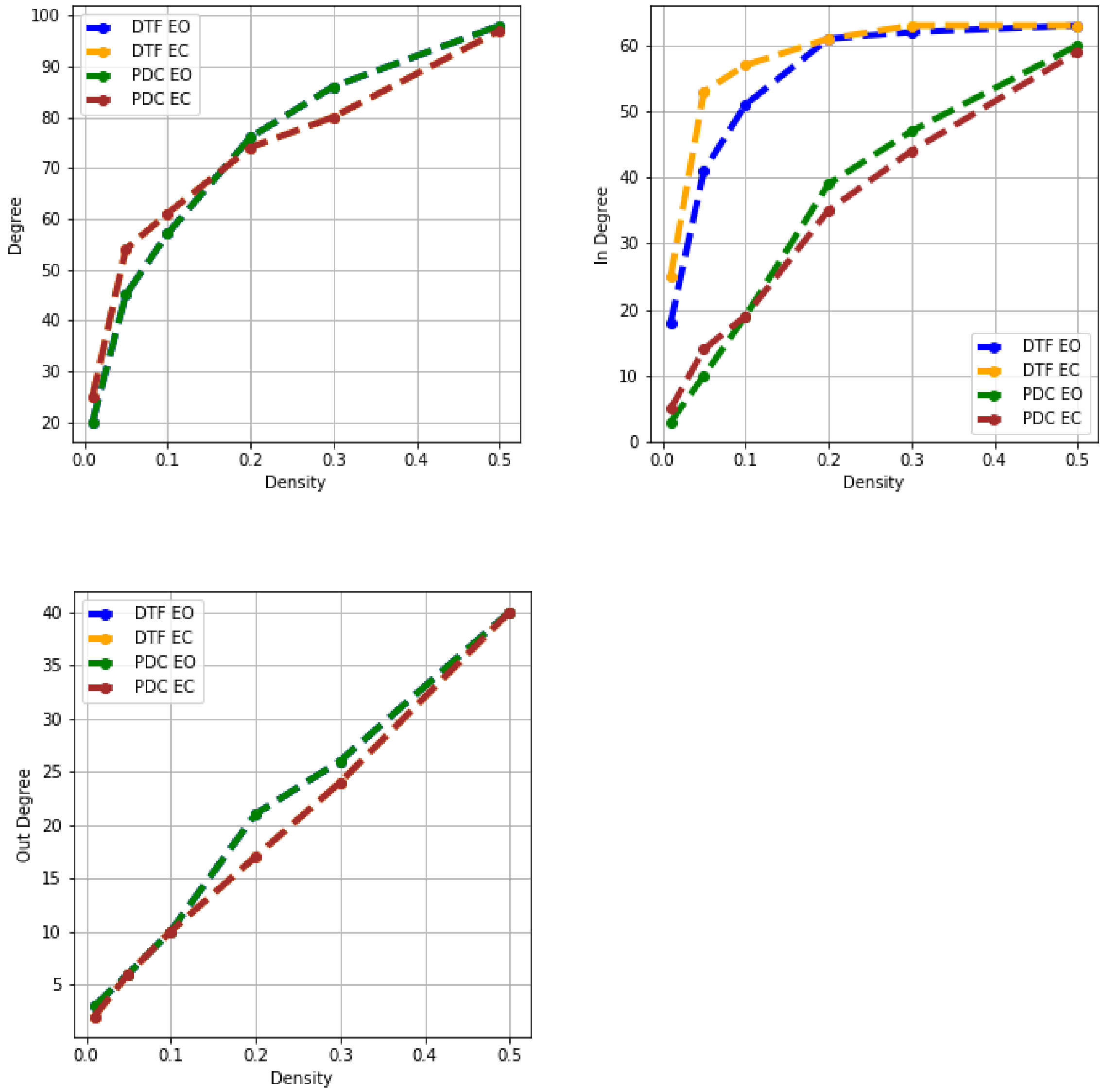

Fig 5.21: Correlation of local indices for both PDC and DTF at different densities

Appendix C: Motif Analysis

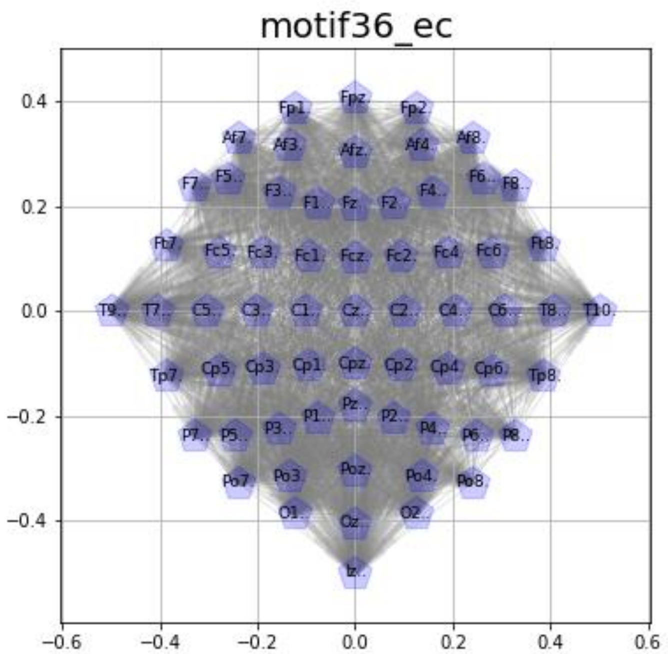

Figure 21: 3-motif Eyes Closed using DTF

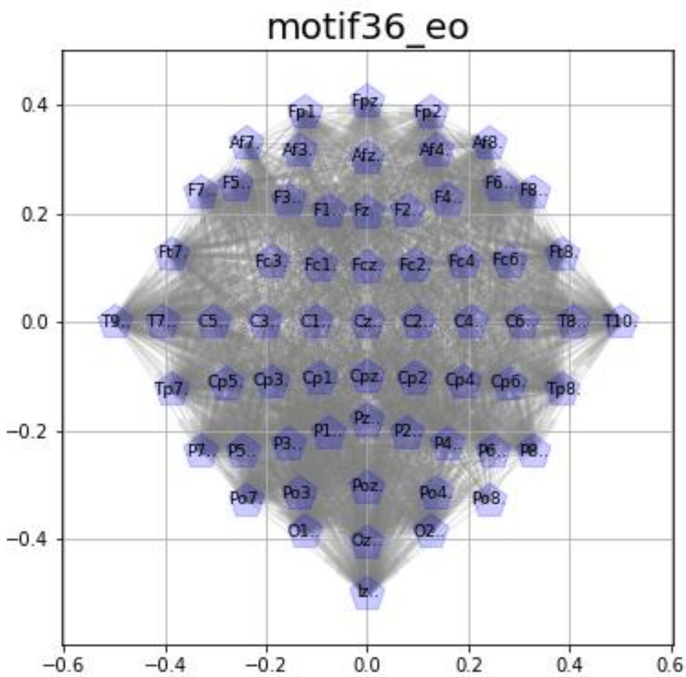

Figure 21: 3-motif Eyes Open using DTF

Appendix D: Community Detection

Community detection using Louvain:

Community ID	Elements	Channels
0	22	Fc6,C3,C2,C4,C6,Cp5,Cp1,Cpz,Cp2,Cp4,Cp6,Tp8,P3,P1,Pz,P2,P4,P6,P8,Po4,Po8,O2
1	17	Fc3,Fcz,Fc4,C1,Cz,Fp1,Fpz,Fp2,Afz,Af4,Af8,F3,Fz,F2,F4,F6,Ft8
2	17	Fc5,C5,Af7,Af3,F7,F5,F8,Ft7,T7,T9,Tp7,P7,P5,Po7,Po3,O1,Iz
3	8	Fc1,Fc2,Cp3,F1,T8,T10,Poz,Oz

Table 1: Communities using Louvain eyes-closed using DTF graph

Community ID	Elements	Channels
0	25	Fc1,C1,Cp5,Cp1,Cpz,Cp2,Cp4,Cp6,T10,Tp8,P7,P5,P1,Pz,P2,P4,P6,P8,Poz,Po4,Po8,O1,Oz,O2,Iz
1	23	Fc5,Fc3,Fcz,Fc2,Fc6,C3,Fp1,Fpz,Fp2,Af7,Af3,Afz,Af4,Af8,F7,F5,F3,F1,F2,F4,F6,F8,Ft7
2	8	Cz,C6,Cp3,Fz,Ft8,T7,T9,Po7
3	3	C5,Tp7,P3
4	2	C4,T8
5	2	C2,Po3
6	1	Fc4

Table 2: Communities using Louvain eyes-open using DTF graph

Community detection using Info map:

Community ID	Elements	Channels
0	55	Fc5,Fc3,Fcz,Fc2,Fc4,Fc6,C5,C3,C1,Cz,C2,C4,C6,Cp5,Cp3,Cp1,Cpz,Cp4,Cp6,Fpz,Fp2,Af7,Af3,Afz,Af4,F7,F5,F3,Fz,F2,F4,F8,Ft7,Ft8,T7,T8,T9,T10,Tp7,Tp8,P7,P5,P3,P1,Pz,P2,P4,P6,P8,Poz,Po4,Po8,Oz,O2,Iz
1	3	Po7,Po3,O1
2	2	Fc1,F1
3	2	Cp2,Fp1
4	2	Af8,F6

Table 3: Communities using Info map eyes-closed using DTF graph

Community ID	Elements	Channels
0	52	Fc1,Fcz,Fc2,Fc4,Fc6,C5,C3,C1,Cz,C4,C6,Cp5,Cp1,Cpz,Cp4,Cp6,Fp1,Fpz,Fp2,Af7,Af3,Afz,Af4,Af8,F1,Fz,F2,F4,F6,F8,Ft7,T8,T10,Tp7,Tp8,P7,P5,P3,P1,Pz,P2,P4,P6,P8,Po3,Poz,Po4,Po8,O1,Oz,O2,Iz
1	5	Fc5,Fc3,F7,F5,F3
2	8	Cz,C6,Cp3,Fz,Ft8,T7,T9,Po7
3	3	Cp3,Ft8,Po7
4	2	T7,T9
5	2	C2,Cp2

Table 4: Communities using Info map eyes-open using DTF graph